NUMERICAL INVESTIGATION OF CONFINEMENT EFFECT ON SUPERSONIC TURBULENT FLOW PAST BACKWARD FACING STEP WITH AND WITHOUT TRANSVERSE INJECTION

P. Manna* and Debasis Chakraborty*

Abstract

Effect of confinement has been investigated numerically for supersonic turbulent flow past backward facing step in a nonreacting scramjet combustor. Flow structure downstream of the backward facing step has been studied by considering various configurations with different combustor heights as well as unconfined flow. Staged transverse sonic injectors with different combustor heights are also considered to find out the effect of confinement on the penetration, spreading and other flow features in the flow field. Three dimensional Navier Stokes equations along with k-ε turbulence model are solved using a commercial CFD software. The simulation captures all essential features of the flow. Good comparisons of various flow profiles have been obtained between experimental and computed values. Although confinement creates complicated shock reflections in the combustor, the length of the recirculation bubble behind the backward facing step remains almost constant. For the injection case, the recirculation region is extended upto the bow shock arising upstream of the injector and two recirculation bubble is seen between the backward facing step and the injector.

Nomenclature

A = coeffieint
h = step height
ER = expansion ratio [= $H/(H-h)$]
H = enthalpy, also height of the combustor
K = turbulent kinetic energy
L = length of the combustor
M = Mach number
P = pressure
Pr = Prandtl number
Q = heat flux
R = residue
S = sutherland constant
S_K,S_ε= source terms for K and ε
t = time
T = temperature
u,v,w= velocity components
X,Y,Z= coordinate axes
W = width of the combustor
ρ = density
τ = shear stress
ε = turbulent kinetic energy dissipation rate
μ = dynamic viscosity
σ_K, σ_ε = coefficient for K and ε equations
λ = thermal conductivity

Suffix

i, j, k = axial direction
ref = reference value
l = laminar
t = turbulent
f*s* = free stream static value

Introduction

The future of air-breathing hypersonic vehicles is largely dependent on the development of efficient propulsion system capable of producing large thrust to overcome the drag of the vehicle. For hypersonic air breathing propulsion with flight Mach number above 6.0, supersonic combustion is indispensable to maintain reasonable temperature and pressure in the combustion chamber and combustion efficiency. Due to supersonic flow speed in the combustion chamber, problems arise in the mixing of reactants, flame anchoring and stability, and completion

* Computational Combustion Dynamics Division, Directorate of Computational Dynamics, Defence Research and Development Laboratory (DRDL), Kanchanbagh Post, Hyderabad - 500 058, India, Email : debasis_cfd@drdl.drdo.in
Manuscript received on 14 Dec 2007; Paper reviewed, revised and accepted on 15 Dec 2008

of combustion within the limited combustion chamber length. Backward facing step [1,2] is employed in the scramjet combustor to stabilize the flame and generate self excited resonance. Hence, a combustor with a transverse injection downstream of a backward facing step is one of the simplest designs to enhance mixing and stabilize the flame simultaneously.

The supersonic flow past a backward facing step in a confined environment is quite complex. The schematic of flow field is shown in Fig.1. The supersonic stream expands at the base corner and the turbulent boundary layer separates and forms a free shear layer that eventually reattaches and undergoes recompression. Between the separation of boundary layer at base corner and the reattachment point, there exists a low speed recirculating flow region which is used for fuel injection and flame stabilization purposes. Because of the complexity of the flow physics, turbulent flow past backward facing step has been considered as a canonical problem in the literature for studying complex turbulent separated flows and many experimental [3-9] and numerical [10-18] investigations were carried out. The sonic transverse injection into the stream further complicates the flow field. As the free stream is blocked partially by the secondary flow, a strong bow shock wave is formed in front of the injection point followed by a barrel shock. Downstream of the injection point, the boundary layer reattaches and a recompression shock wave is generated.

A number of numerical simulations were carried out by solving the Navier Stokes equations to analyse turbulent supersonic flows past backward facing step in free [10-13] and confined supersonic environment [14-18]. Sahu [11] simulated numerically the experimental condition of Herrin and Dutton [7] using 3-D N-S equations. Performance of algebraic and *k*-ε models in predicting turbulent supersonic flow past backward facing step were evaluated and it was concluded that the algebraic models perform poorly in predicting the flow properties in the recirculation zone. Childs and Caruso [12] have included the Mach number effects in the *k*-ε model to obtain a good match with the experimental data for turbulent base flows. Recently, Forsythe et al. [13,14] have applied Detached Eddy Simulation to study the unconfined supersonic base flows and captured most of the flow physics present in the problem of Uenishi et al. [15]. Correa and Warren [16] adopted explicit McCormack scheme to study the backward facing step flow with and without injection of air downstream of the step. Yang et al. [17] employed a flux vector splitting lower-upper symmetric successive over-relaxation scheme and demonstrated that reduction of base pressure and recirculation zone could cause difficulties in injection and flame holding in scramjet combustor. Supersonic flow over a backward facing step corresponding to the experimental condition of Hartfield et al. [5] was analysed by Yang [18] using a hybrid (structured near the wall and unstructured in the far field) and adaptive grid using an Euler solver. The mixing characteristics of sonic air injection in supersonic streams behind a backward facing step is simulated numerically by Manna and Chakraborty [19] using a 3D Navier Stokes equations and *k*-ε turbulence model. Good agreement is obtained between experimental and the computed values for the injectant spreading and penetration as well as for various flow properties.

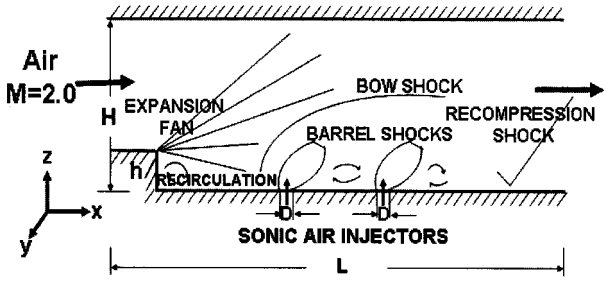

Fig.1 Schematic of Flow Field

In scramjet combustor, the flow field in region of backward facing step is subjected to lateral confinement which may alter the shear layer structures, barrel shocks, reattachment point, the recompression shock and its reflection from the top wall. The effect of lateral confinement has not been addressed adequately in literature for supersonic flow in scramjet combustor. The expansion ratio, *ER=H/H-h*, *H* and *h* being the combustor height and step height respectively, may be an important parameter for finding out the flow field structures.

In this work, the experimental conditions of supersonic flow past backward facing step for free [3] and confined environment [4] has been simulated using a commercial CFD software CFX-TASCflow [20] and various flow profiles are compared. The effect of confinement on the flow structure with and without injection is studied numerically for different heights of the combustor geometry.

Methodology

CFX-TASCflow [20] is an integrated software system capable of solving diverse and complex multidimensional fluid flow and heat transfer problems. The software solves three dimensional Reynolds Averaged Navier Stokes (RANS) equations in a fully implicit manner. It is a finite volume method and is based on a finite element approach to represent the geometry. The method retains much of the geometric flexibility of finite element methods as well as the important conservation properties of the finite volume method. It utilizes numerical upwind schemes to ensure global convergence of mass, momentum, energy and species. It implements a general non-orthogonal, structured, boundary fitted grids. In the present study, the discretisation of the convective terms is done by first order upwind difference scheme. The turbulence model used was *k*-ε model with wall functions.

Governing Equations

The appropriate system of equations governed the turbulent compressible gas may be written as

Continuity equation:

$$\frac{\partial \rho}{\partial t} + \frac{\partial}{\partial x_k}(\rho\, u_k) = 0 \qquad k = 1, 2, 3$$

Momentum Equation:

$$\frac{\partial}{\partial t}(\rho\, u_i) + \frac{\partial}{\partial x_k}(\rho\, u_i\, u_k) + \frac{\partial p}{\partial x_i} = \frac{\partial(\tau_{ik})}{\partial x_i}, \qquad i, k = 1, 2, 3$$

Energy Equation:

$$\frac{\partial}{\partial t}(\rho H) + \frac{\partial}{\partial x_k}(\rho\, u_i H) = \frac{\partial}{\partial x_k}(u_j\, \tau_{jk}) + \frac{\partial q_k}{\partial x_k}, \qquad j, k = 1, 2, 3$$

Turbulent kinetic energy (*k*) equation:

$$\frac{\partial}{\partial t}(\rho k) + \frac{\partial}{\partial x_k}(\rho\, u_k\, k) = \frac{\partial}{\partial x_k}\left(\left(\frac{\mu_l}{\mathrm{Pr}} + \frac{\mu_t}{\sigma_k}\right)\frac{\partial k}{\partial x_k}\right) + S_k$$

Rate of dissipation of turbulent kinetic energy (ε) equation:

$$\frac{\partial}{\partial t}(\rho\, \varepsilon) + \frac{\partial}{\partial x_k}(\rho\, u_k\, \varepsilon) = \frac{\partial}{\partial x_k}\left(\left(\frac{\mu_l}{\mathrm{Pr}} + \frac{\mu_t}{\sigma_\varepsilon}\right)\frac{\partial \varepsilon}{\partial x_k}\right) + S_\varepsilon$$

where, ρ, u_i, *p*, *H* are the density, velocity components, pressure and total energy respectively and $\mu = \mu_l + \mu_t$ is the total viscosity; μ_l, μ_t being the laminar and turbulent viscosity and *Pr* is the Prandtl number. The source term S_K and S_ε of the *K* and ε equation are defined as

$$S_k = \tau_{ik}\frac{\partial u_i}{\partial x_k} - \rho\,\varepsilon \quad \text{and} \quad S_\varepsilon = C_{\varepsilon 1}\,\tau_{ik}\frac{\partial u_i}{\partial x_k} - C_{\varepsilon 2}\frac{\rho \varepsilon^2}{k}$$

where turbulent shear stress is defined as

$$\tau_{ik} = \mu_t\left(\frac{\partial u_i}{\partial x_k} + \frac{\partial u_k}{\partial x_i}\right)$$

Laminar viscosity (μ_l) is calculated from Sutherland law as

$$u_l = \mu_{ref}\left(\frac{T}{T_{ref}}\right)^{3/2}\left(\frac{T_{ref} + S}{T + S}\right)$$

where, T is the temperature and μ_{ref}, T_{ref} and *S* are known coefficient. The turbulent viscosity μ_t is calculated as

$$\mu_t = c_\mu \frac{\rho k^2}{\varepsilon}$$

The coefficients involved in the calculation of μ_t are taken as

$c_\mu = 0.09, \quad C_{\varepsilon 1} = 1.44, \quad C_{\varepsilon 2} = 1.92$

$\rho_\kappa = 1.0, \quad \sigma_\varepsilon = 1.3, \quad \sigma_c = 0.9$

The heat flux q_k is calculated as $q_k = -\lambda\frac{\partial T}{\partial x_k}$, λ is the thermal conductivity

Discretisation of Governing Equations

The CFX-TASCflow solver utilizes a finite volume approach, in which the conservation equations in differential form are integrated over a control volume described around a node, to obtain an integral equation. The pressure integral terms in momentum integral equation and the spatial derivative terms in the integral equations are evaluated using finite element approach. An element is described with eight neighboring nodes. The advective term is evaluated using upwind differencing with physical advection correction. The set of discretised equations form a set of algebraic equations: $A\ \vec{x} = b$ where $\vec{x}$ is the solution vector. The solver uses an iterative procedure to update an approximated x_n (solution of x at n^{th} time level) by solving for an approximate correction x' from the equation $A\ \vec{x}' = \vec{R}$, where $\vec{R} = \vec{b} - A\vec{x}_n$ is the residual at n^{th} time level. The equation $A\ \vec{x}' = \vec{R}$ is solved approximately using an approach called Incomplete Lower Upper factorization method. An algebraic multigrid method is implemented to reduce low frequency errors in the solution of the algebraic equations. Maximum residual $\left(= \phi_j^{n+1} - f\left(\phi_j^{n+1}, \phi_j^{n}\right)\right) < 10^{-4}$ is taken as convergence criteria.

Results and Discussions

Unconfined Supersonic Flow Past Backward Facing Step

Simulations are first carried out for the experimental condition [3] of unconfined supersonic flow past a backward facing step. The supersonic flow of Mach 2.0 with static pressure of 39 kPa and temperature of 170 K passes over a backward facing step of 3.2 mm height. In the simulation, X axis is taken along the length of the combustor while Y and Z axis are taken along the width and the height of the combustor respectively. The origin of the coordinate system is located at the bottom center of the step. A total of 129x3x87 gridpoints are used in the simulation. The grids are fine near the wall and backward facing step region and relatively coarse in the outward region. The grid independence of the results are demonstrated by comparing the axial distribution of surface pressure for three different grids, namely, 109x3x72, 129x3x87 and 157x3x104 in Fig.2. It can be seen that by changing the number of gridpoints from 109x3x72 to 157x3x104 the results do not change appreciably. The Mach number distribution in X-Z plane is shown in Fig.3 to describe the qualitative features of the flow. The expansion at the base corner, reattachment of shear layer and

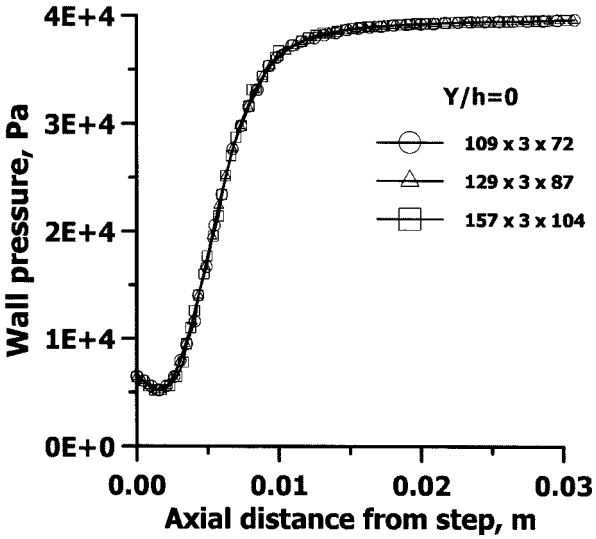

Fig.2 Grid Independence Study

Fig.3 Velocity Vector Plot and Mach Number Distribution in X-Z Plane

recirculation of flow and recompression shocks are clearly visible in the figure. The blown-up view of the velocity vector near the backward facing step is shown to depict the recirculation pattern. The computed pressure profile at X/h=7.0 has been compared with the experimental results and the numerical results of Uenishi et al. [15] in Fig.4. A good match between the three has been obtained.

Confined Supersonic Flow over Backward Facing Step

McDaniel et al. [4, 5] have conducted experimental investigations for a Mach 2.0 supersonic airflow over a backward facing step combustor with a step height of 3.2 mm. The measurement (PLIIF and LIIF) of various flow parameters at various axial locations of the combustor are presented in detail. The length, height and width of the combustor are 91.02 mm, 21.29 mm and 30.48 mm respectively. The backward facing step is provided to generate

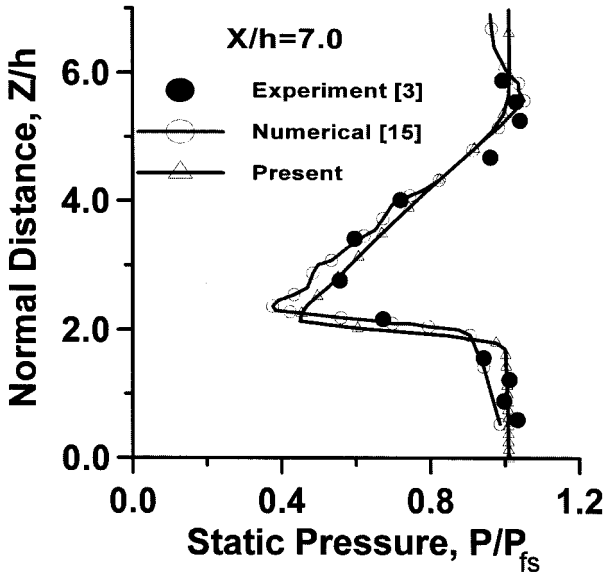

Fig.4 Static Pressure Comparison

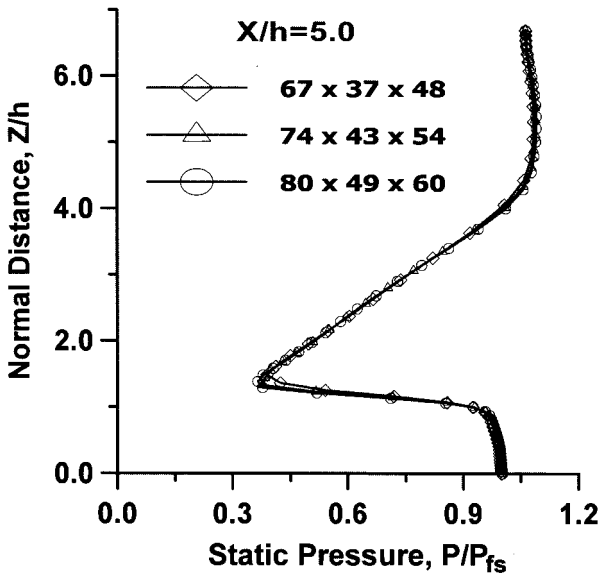

Fig.5 Pressure Profiles at X/h = 5.0 with three Different Grid

low pressure recirculation zone to choose an injection region for flame holding in supersonic flow. The geometrical details and the inflow conditions of the combustor geometry are summarized in Table-1.

The inflow boundary is taken at 11.02 mm upstream from the step and the outflow boundary is set at 80 mm downstream along the flow direction. A non-uniform stretched structured grid of 80x49x60 is taken for the present computation. Very fine grids, minimum of the order of 0.1 mm (Y^+ ~15.0) are provided adjacent to the step and near wall region and the grids are relatively coarser in other regions. Simulations are carried out for three different grids, namely, 67x37x48, 74x43x54 and 80x49x60. The comparison of pressure distribution with three different grids for without injection case at X/h=5.0 in Fig.5 shows that the results do not change by changing the grid from 67x37x48 to 80x49x60, thus proving the grid independence of the results.

Comparison of Flow Parameters with and without Injection

Velocity vector plot with streamline and pressure distribution have been plotted in X-Z plane for without injection case in Fig.6. The expansion fan, reattachment and recompression by the oblique shockwave are clearly visible. The recompression shockwave is reflected back from the top wall towards the bottom wall near the exit of the combustor. The flow behavior in low pressure recirculation region adjacent to backward facing step is compared with and without injection case in Fig.7. A single recirculation bubble and the reattachment point at the end of the recirculation bubble for without injection case are crisply visible. The reattachment point is defined as the location where the separated shear layer reattaches to the bottom surface and is determined where the surface velocity is zero. The surface velocity is defined as the streamwise velocity component measured very close to the surface. In the present case, the location for the measurement has been

Table-1 : Geometrical and Inflow Details of the Computational Domain

Geometrical Parameters	**Value**	**Inflow Parameters**	**Value**
Test Section length, L (mm)	91.02	Static pressure, P_{fs} (kPa)	35.0
Test Section height, H (mm)	21.29	Static temperature, T_{fs} (K)	167.0
Test Section width, W (mm)	30.48	Mach number, M	2.0
Step height, h (mm)	3.2	Axial velocity, u_{fs} (m/s)	518.1
Step location, X (mm)	0.0	Molecular weight	28.8

Fig.6 Velocity Vector Plot and Pressure Distribution in X-Z Plane

Fig.7 Velocity Vectors Adjacent to the Backward Facing Step

taken at 0.1 mm above (Z = 0.1 mm) the bottom surface. The average value of the reattachment point (X_R) for without injection case is about 2.03h measured from the step of the combustor. This value is lower compared to the subsonic turbulent flow as reported by Eaton and Johnston [21]. The reattachment length is fairly constant along the

Fig.8 Axial Velocity Distribution Adjacent to Backward Facing Step

width of the combustor. For the injection case, the recirculation zone is extended upto bow shock caused due to injection. The flow pattern in the base region is different for with and without injection case. For injection case, two distinct recirculation bubbles are seen in the base region

compared to the single recirculation bubble for the without injection case. Velocity vector distributions in three different planes along the width (Y/h=0.0, 2.0 and 4.0) are compared between the transverse injection and without injection case in Fig.8 for the combustor height H/h=6.65. The shape of the recirculation bubble in X-Y plane is also shown in the same figure. For without injection case, the velocity vectors in all the three planes are similar and there is almost no variation of the recirculation bubble along the width of the combustor. For the injection case, velocity vector distributions differ significantly between the injection plane and off-injection planes. In the injection plane, the recirculation bubble is extended up to shock and two distinct vortical structures are seen whereas in the off-injection planes the flow is almost similar to the without injection case. Significant variation of the reattachment length is seen along the width. From detailed examination of the numerical results, it has been found that at Y/h=2.3, the reattachment length matches with that of without injection case. The computed nondimensional axial velocity (u) profiles for without injection case at three different axial locations, namely, X/h=1.75, 3.0 and 6.66 are compared with the experimental value [4] in Fig.9. Velocity has been nondimensionalised by the free stream axial velocity (u_{fs}) and the combustor height (H) is nondimensionalised by step height (h). The compared velocity profiles match extremely well with the experimental values for all the three axial locations. The computed nondimensional pressure and temperature profiles are compared with the experimental values in Fig.10 and Fig.11 respectively. Pressure and temperature are nondimensionalised by their respective free stream values. Pressure profiles match with the experimental results away from the lower surface (Z/h > 1.0). Near the wall region (Z/h < 1.0), there are differences between the experimental and computational values. In fact, two measurement techniques (PLIIF) and (LIIF) show considerable differences in the near wall region (Z/h < 1.0) showing the complex nature of the flow. The temperature profiles at three locations show reasonable agreement with the experimental values.

Effect of Confinement on the Flow Parameters

The effect of confinement on the supersonic turbulent flow behind the backward facing step is studied by simulating the combustor geometry with different heights (H). Six expansion ratios [$ER = H/(H\text{-}h)$] varying from 1.177 to 2.0 were simulated along with unconfined flow. In all the cases, the length and the width of the combustor and inflow parameters are kept constant, whereas, the height

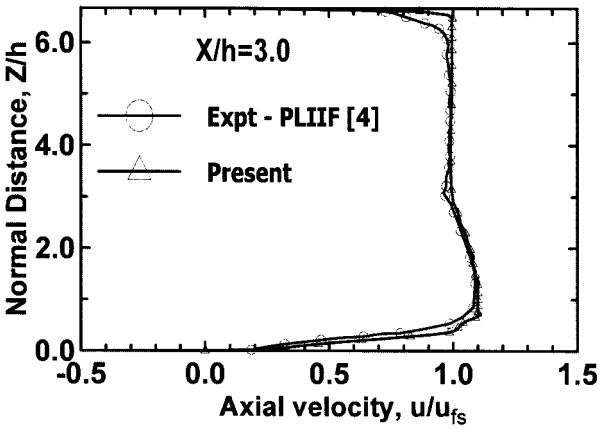

Fig.9b Axial Velocity Distribution at X/h = 3.0

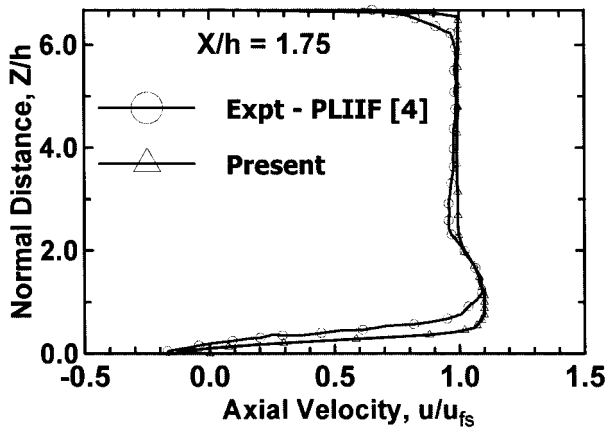

Fig.9a Axial Velocity Distribution at X/h = 1.75

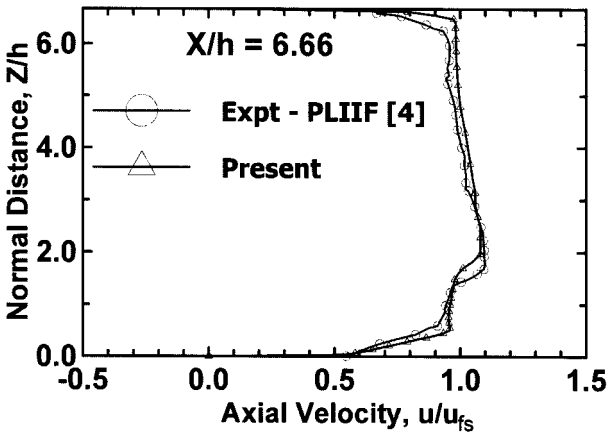

Fig.9c Axial Velocity Distribution at X/h = 6.66

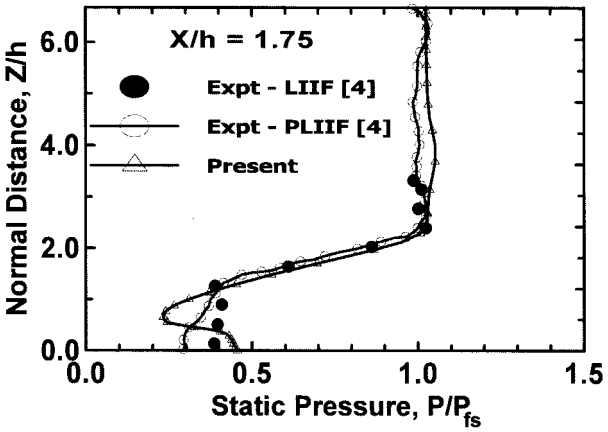

Fig.10a Pressure Distribution at X/h = 1.75

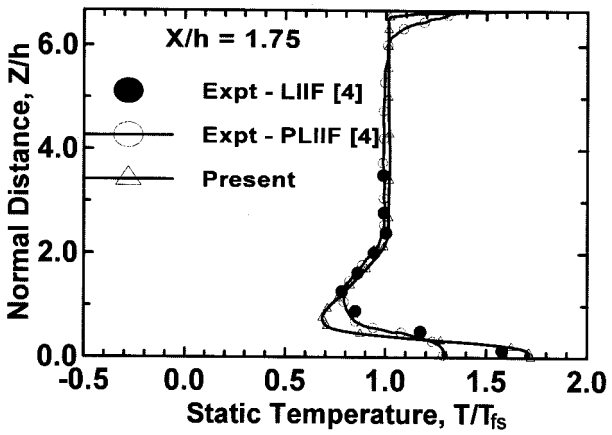

Fig.11a Temperature Distribution at X/h = 1.75

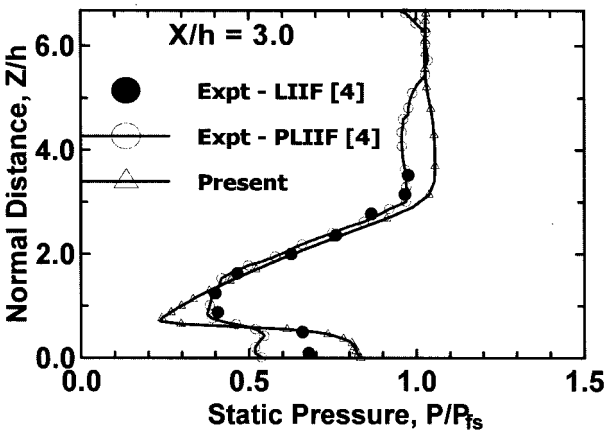

Fig.10b Pressure Distribution at X/h = 3.0

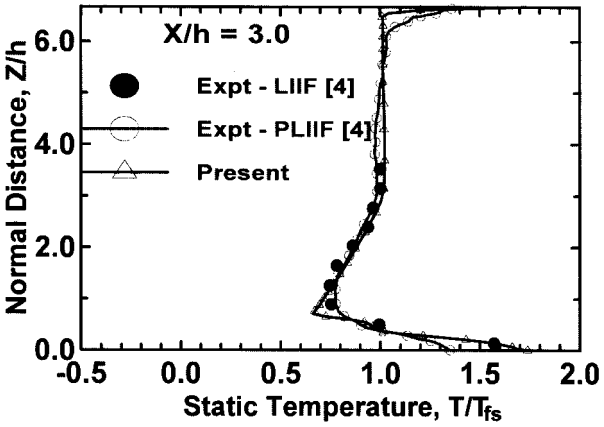

Fig.11b Temperature Distribution at X/h = 3.0

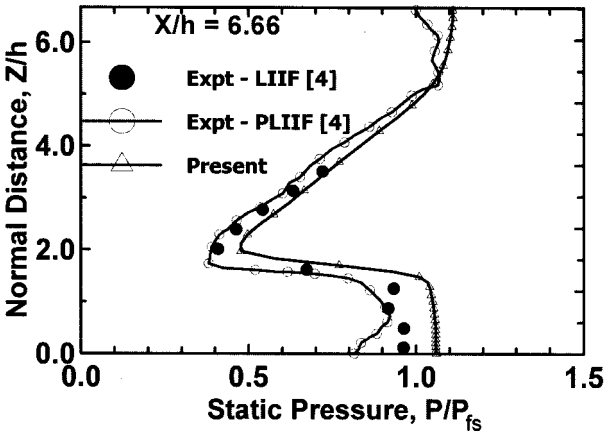

Fig.10c Pressure Distribution at X/h = 6.66

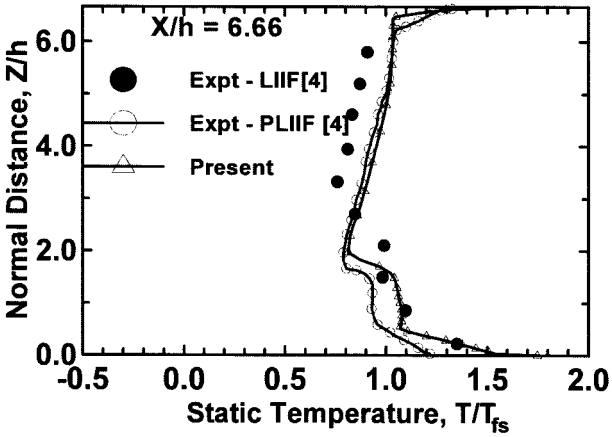

Fig.11c Temperature Distribution at X/h = 6.66

Table-2 : Expansion Ratio for Simulation				
Sl. No.	**Height of the Combustor including Step, H (mm)**	**Height of the Step, h (mm)**	**Ratio of H/h**	**Expansion Ratio, ER = H/(H-h)**
1.	6.4	3.2	2.0	2.0
2.	9.6	3.2	3.0	1.5
3.	12.8	3.2	4.0	1.33
4.	16.0	3.2	5.0	1.25
5.	19.2	3.2	6.0	1.20
6.	21.28	3.2	6.65	1.177
7.	Unconfined	3.2	$\sim \alpha$	~ 1.0

of the combustor has been varied. The details of the geometrical parameters are presented in Table-2.

The flow characteristics in terms of pressure distribution for various expansion ratios are shown in Fig.12. The recompression shockwave angle is almost same for all the cases and is measured to be about 21° with respect to the bottom wall. With the increase of the combustor height, the number of shock reflections has been seen to decrease. For the smallest height of the combustor (H=2h) the shock wave train terminates near the exit of the combustor where the flow becomes almost uniform. The number of reflections depends on the height of the geometry. For H=2h, the number of reflection is five compared to four for H=3h and two for H=6.66h. The same features are also visible in the axial pressure distribution plot for top and bottom wall in Fig.13. The value of pressure is almost same at the exit and equals to approximately 0.58 P_{fs} for both top and bottom wall for H/h=2.0. Confinement does not affect the flow structure in the recirculating region behind the backward facing step at all. The pressure distribution at the bottom wall follow the unconfined value up to X/h=4.0. For the lowest height of the combustor geometry (ER=2.0), the reflection shock hits the bottom wall only at X/h=8.0 whereas, the reattachment length is X/h=2.038.

The comparisons of numerical and experimental values of various flow parameters including spreading and penetration of the sonic transverse jet for different dynamic pressure ratio of the two streams are reported by the

Fig.13a Pressure Distribution on Bottom Wall

Fig.12 Pressure Distribution for Different Expansion Ratio

Fig.13b Pressure Distribution on Top Wall

same authors [19]. The effect of the confinement on the penetration and spreading and other flow properties are studied in the present work by carrying out the simulations with different combustor heights. The geometry and inflow parameters are explained in Table-1. Two sonic air jets of 2.0 mm diameter each are placed at middle of the bottom plate at X/h=4.0 and 8.0 from the step. The jet static pressure and temperature are 140 kPa and 248 K respectively. The penetration and spreading are presented are compared in Fig.14 for with and without injection. The spreading of the sonic jet has not been affected at all by confinement. For, H/h=3.0, the sonic jet is found to hit the top wall. For other two cases, the effect of confinement on penetration is very marginal. The axial distribution of top wall and bottom wall pressures for with and without injection case are compared in Fig.15 for the confinement ratios (H/h) of 3.0, 5.0 and 6.65. The surface pressure distributions on both the walls are seen to be quite different between the injection and without injection case. The lateral distribution of pressures at X/h=2.0, 3.0, 5.0, 6.0 and 11.0 are compared between the injection and without injection for H/h=6.65 case and is shown in Fig.16. The spanwise average value of reattachment length from the step is calculated and plotted in non-dimensional form in Fig.17. The reattachment length slightly increases with the height of the combustor upto H/h=4.0. Then it decreases gradually to almost constant value to 2.03 at higher H/h ratio as well as for unconfined flow.

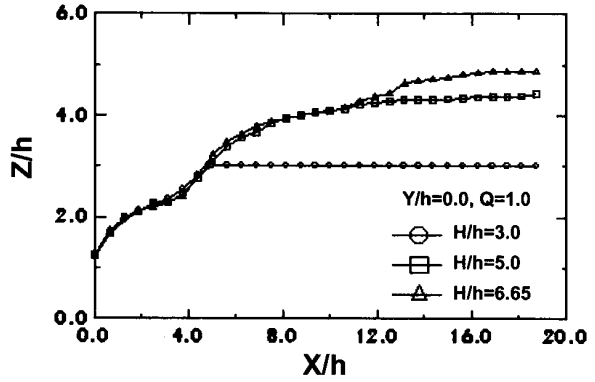

Fig.14a Injectant Penetration

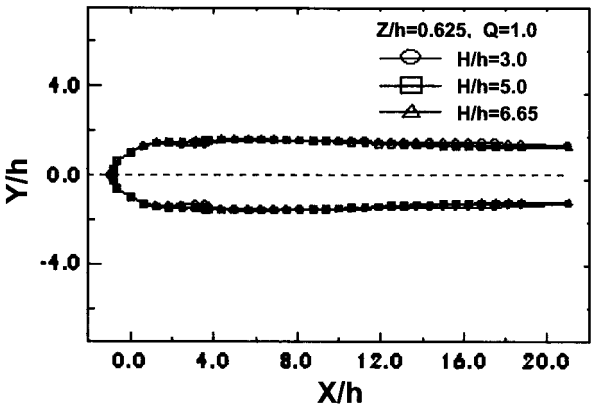

Fig.14b Injectant Spreading Distribution

Conclusions

Numerical simulations are presented to study the effect of confinement for supersonic turbulent flow past backward facing step in a nonreacting scramjet combustor. Three dimensional Navier Stokes equations are solved along with k-ε turbulence model using a commercial CFD software. Grid independence of the results is established by comparing flow profiles with different grids. The simulation captures all the essential features of the flow field and the computed profiles of various flow parameters matches well with the experimental results at different axial stations. The results obtained for different combustor heights with sonic transverse injection into the supersonic stream are compared with that of without injection to find out the effect confinement on the flow development proc-

Fig.15a Pressure Distribution on Bottom Wall

Fig.15b Pressure Distribution on Top Wall

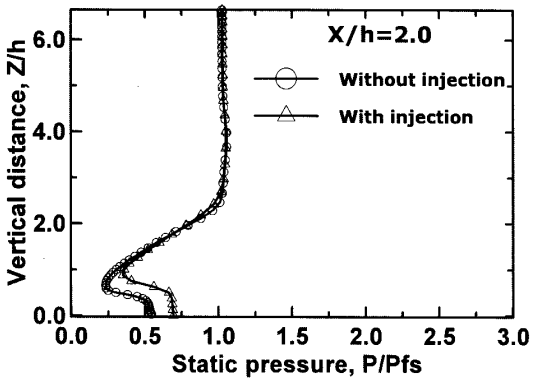

Fig.16a Transverse Pressure Profiles at X/h = 2.0

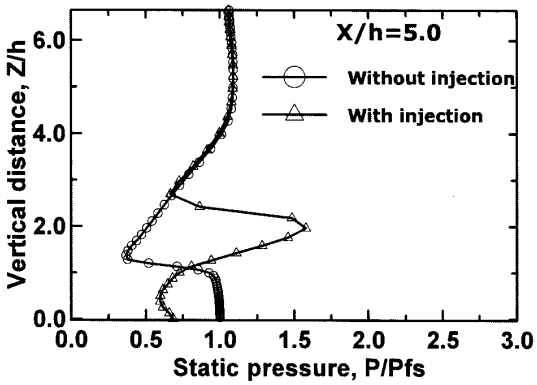

Fig.16c Transverse Pressure Profiles at X/h = 5.0

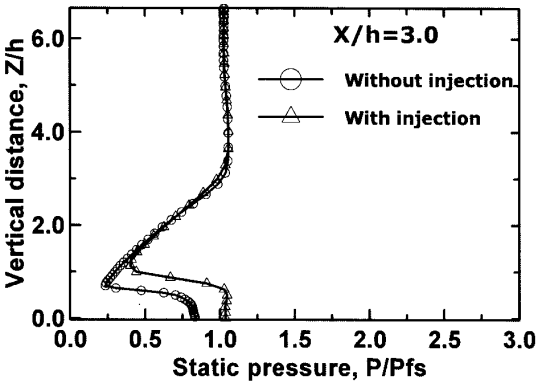

Fig.16b Transverse Pressure Profiles at X/h = 3.0

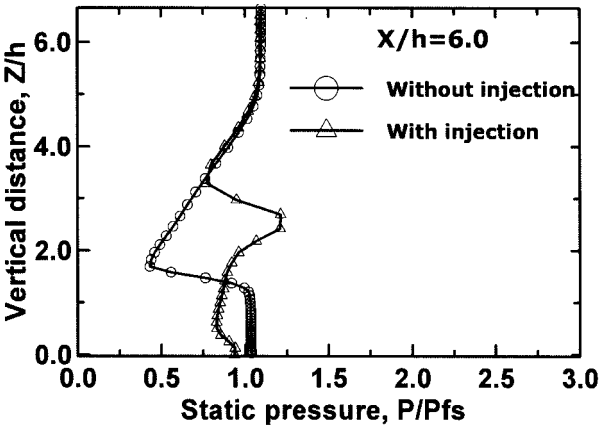

Fig.16d Transverse Pressure Profiles at X/h = 6.0

ess. For without injection, although the confinement generates a complicated shock reflection pattern in the combustor, the length of the recirculation bubble behind the backward facing step almost remains constant. For transverse sonic injection, confinement does not seem to effect the penetration and spreading of the injectant significantly. The recirculation flow behind the backward facing step is extended upto the bow shock arising due to injectors. The structure of the recirculation bubble behind the backward facing step is seen to be different in shape and size between the two cases. For without injection case, single recirculation bubble with constant width is seen, whereas, two separate recirculating structures with significant variations along the width is seen for the injection case.

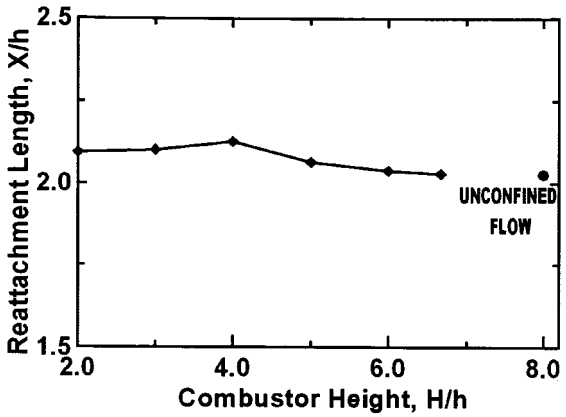

Fig.17 Reattachment Length Vs. H/h Ratio

References

1. Gutmark, E., Wilson, K.J., Schadow, K.C., Parr, T.P. and Hanson-Parr, D.M., "Combustion Enhancement in Supersonic Co-axial Flow", AIAA Paper 89-2788, 1989.

2. Yu, K., Wilson, K.J. and Schadow, K.C., "On the Use of Combustor Wall Cavities for Mixing Enhancement", Third American Society of Mechanical Engineers, Paper 99-7255, 1999.

3. Fletcher, D.G. and McDaniel J.C., "Quantitative Measurement of Transverse Injector and Free Stream Interaction in a Nonreacting Scramjet Combustor Using Laser Induced Fluorescence", AIAA Paper 87-0087, 1987.

4. McDaniel, J.C., Fletcher, D.G., Hartfield R.J. and Hollo, S.D., "Staged Transverse Injection into Mach 2 Flow Behind a Rearward-Facing Step: A 3-D, Compressible Flow Test Case for Hypersonic Combustor CFD Validation", AIAA Paper 92-0827, 1992.

5. Hartfield R.J., Hollo, S.D and McDaniel, J.C., "Planar Measurement Technique for Compressible Flows Using Laser Induced Iodine Fluorescence", AIAA Journal, Vol.31, No.3, 1993, pp.483-496.

6. Dutton, J.C., Herrin, J.L., Molezzi, M.J., Mathur, T. and Smith, K.M., "Recent Progress on High Speed Separated Base Flows", AIAA Paper 93-0472, 1993.

7. Herin, J.L. and Dutton, J.C., "Supersonic Base Flow Experiments in the Near Wake of a Cylinder Afterbody", AIAA Journal, Vol.32, No.1, 1994, pp.77-83.

8. Herrin, J.L. and Dutton, J.C., "An Investigation of LDV Velocity Bias Correction Technique for High Speed Separated Flows", Experiments in Fluids, Vol.15, No.4/5, 1993, pp.354-363.

9. Kuratani, N., Ikeda, Y., Nakajima, T., Tomioka, S. and Mitano, T., "Mixing Characteristics of Normal Injection into a Supersonic Backward Facing Step Flow Measurement with PIV", AIAA Paper 2002-0237, 2002.

10. Smith, K.M. and Dutton, J.C., "Investigation of Large Scale Simulation in Supersonic Planar Base Flows", AIAA Journal, Vol.34, No.4, 1996, pp.1146-1152.

11. Sahu J.L., "Numerical Computation of Supersonic Base Flow with Special Emphasis on Turbulence Modeling", AIAA Journal, Vol.32, No.7, 1994, pp.1547-1549.

12. Childs, R.E. and Caruso, S.C., "On the Accuracy of Turbulent Base Flow Prediction", AIAA Paper 87-1939, 1987.

13. Forsythe, J.R. and Hoffman, K.A., "Detached-Eddy Simulation of a Supersonic Axisymmetric Base Flow with an Unstructured Solver", AIAA Paper 2000-2410, 2000.

14. Forsythe, J.R., Hoffman, K.A. and Squires K.D., "Detached-Eddy Simulation with Compressibility Corrections Applied to Supersonic Axisymmetric Base Flow", AIAA Paper 2002-0586, 2002.

15 Uenishi, K., Rogers, R.C. and Northam G.B., "Numerical Predictions of a Rearward-Facing-Step Flow in a Supersonic Combustor", Journal of Propulsion and Power, Vol.5, No.2, 1989, pp.58-164.

16. Correa, S.M. and Warren, R.E., "Supersonic Sudden Expansion Flow with Fluid Interaction: An Experimental and Computational Study", AIAA Paper 89-0389, 1989.

17. Yang, A.S., Hscih, W.H. and Kuo, K.K., "Theoretical Study of Supersonic Flow Separation over a Rearward Facing Step", AIAA Paper 91-2161, 1991.

18. Yang, A.S., "Adaptive Refinement of a Supersonic Flow over a Backward Facing Step", AIAA Paper 2001-3741, 2001.

19. Manna, P. and Chakraborty, D., "Numerical Investigation of Transverse Sonic Injection in Non-reacting Supersonic Combustor", Proc. IMechE Part G: J. Aerospace Engineering, Vol.219, No.3, 2005, pp.205-215.

20. CFX-TASCflow Computation Fluid Dynamics Software, Version 2.11.1, AEA Technology Engineering Software Ltd. 2001.

21. Eaton, J.K. and Johnston, J.P., "Review of Research on Subsonic Turbulent Flow", AIAA Journal, Vol.19. 1981, pp.1093-1100.